

Cite this: *Chem. Sci.*, 2025, 16, 5688

All publication charges for this article have been paid for by the Royal Society of Chemistry

Multimeric, multivalent fusion carrier proteins for site-selective glycoconjugate vaccines simultaneously targeting *Staphylococcus aureus* and *Pseudomonas aeruginosa*[†]

Charlotte Sorieul,^{ab} Bartal Mikladal,^{‡b} Dung-Yeh Wu,^{ab} Barbara Brogioni,^b Cinzia Giovani,^b Giusy Adamo,^b Giacomo Romagnoli,^b Immaculada Margarit Y Ros,^{ib} Jeroen Codée,^{ib} Maria R. Romano,^b Filippo Carboni^{*b} and Roberto Adamo^{ib}*

Staphylococcus aureus and *Pseudomonas aeruginosa* are major antimicrobial-resistant pathogens that often synergize in polymicrobial infections, such as chronic wound infections. These notorious and increasingly resistant bacteria contribute significantly to reduced antibiotic efficacy. Despite their substantial clinical burden, the urgent need to combat bacterial resistance and extensive research efforts, no vaccines currently exist for either bacterium. Glycoconjugate vaccines, which extend the range of suitable vaccine antigens to bacterial carbohydrates, could play a major role in this emergence. This study introduces a multiepitope vaccine conjugating *S. aureus* capsular polysaccharide serotype 8 to a chimeric protein fusing Hla and PcrV, two potent cytotoxins from *S. aureus* and *P. aeruginosa*, respectively. A conjugation strategy based on selective targeting of a purposefully introduced histidine tag was developed to preserve the structure and antigenicity of epitopes from the two proteins, leveraging their dual role as a carrier and antigen. This multivalent, multimeric and multipathogen construct successfully elicited antibodies against all three antigens as well as functional protection. This proof-of-concept highlights the potential for advanced vaccines targeting polymicrobial infections and bacteria with complex pathogenesis calling for multivalent formulations. It also points out the power of site-selective conjugation as a tool for vaccine manufacturing.

Received 20th December 2024
Accepted 20th February 2025

DOI: 10.1039/d4sc08622h

rsc.li/chemical-science

Introduction

Staphylococcus aureus and *Pseudomonas aeruginosa* currently stand as two of the leading antimicrobial-resistant (AMR) pathogens, driving antibiotic drug inefficiency and persistent infections.^{1–3} *P. aeruginosa* is an ubiquitous Gram-negative bacterium known for causing severe hospital-acquired infections⁴ with a mortality rate of 37%.^{5,6} It can lead to acute ventilator-associated pneumonia,^{7,8} is a known colonizer in chronic obstructive pulmonary disease and causes chronic infections in cystic fibrosis patients,⁴ leading to progressive lung decline.^{9,10} In the case of chronic wound infections, *P. aeruginosa* has been shown to synergize with other bacteria, primarily *S. aureus*.^{11,12} *S. aureus* is a Gram-positive commensal

bacterium, with a bacteremia mortality rate of about 18% in developed countries, and even higher in developing regions.¹³ It is the leading cause of nosocomial and community-acquired skin and soft tissue infections¹⁴ and surgical site infections.¹⁵ Both pathogens are classified as serious threats by the Centers for Disease Control and Prevention,² and combating their infections remains a global challenge. However, despite decades of vaccine development, no effective preventive intervention is currently licensed for either bacterium.

Glycoconjugate vaccines offer a promising and safe approach to turn poorly immunogenic bacterial surface glycans into effective antigens by their covalent linkage to so-called protein carriers. These carriers provide epitopes capable of eliciting T cell help, thereby fostering a durable and buildable immune protection.^{16–19} Considering the complexity of bacterial pathogenesis and the multitude of virulence factors, as is the case for *S. aureus* and *P. aeruginosa*, a multiepitope approach, in which different antigens are simultaneously incorporated, is considered more promising for effective vaccines.²⁰ Chemical glycoconjugation provides a prime opportunity for the coupling of several antigens, conveniently packed into a single construct

^aLeiden Institute of Chemistry, Leiden University, Einsteinweg 55, 2333 CC Leiden, Netherlands

^bGSK Siena, Via Fiorentina, 1, 53100 Siena SI, Italy. E-mail: roberto.x.adamo@gsk.com; filippo.x.carboni@gsk.com

[†] Electronic supplementary information (ESI) available. See DOI: <https://doi.org/10.1039/d4sc08622h>

[‡] Current address: Genmab BV, Uppsalalaan 15, 3584 CT Utrecht, Netherlands

In this work, we present a novel strategy to generate a multivalent, multimeric vaccine targeting two different pathogens by generating fusion proteins, composed of several copies of Hla and PerV, as a carrier for the site-selective conjugation of

The summary of the tetramer production can be found in Table 1. PcrV was easily expressed in soluble form, while Hla_{H35L} showed a tendency to aggregate in inclusion bodies (Fig. S1[†]). As a result, the presence of Hla_{H35L} in the case of P2H2 reduced both the expression levels and the solubility of the tetramer. Sonication was found to be the most suitable lysis

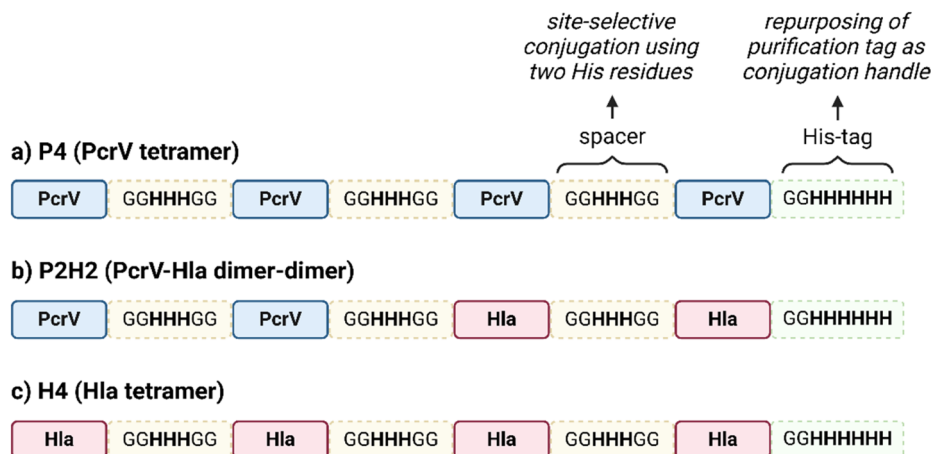


Fig. 1 Schematic representation of the tetrameric fusion protein carriers with histidine (His₃) spacers (in yellow) in between protein copies to serve as conjugation handles; a His₆-tag (in green) is also present, both for purification and conjugation purposes; (a) PcrV fusion tetramer (P4), composed of 4 PcrV copies (in blue); (b) PcrV and Hla hybrid dimer–dimer with His₃ spacers (P2H2); (c) Hla fusion tetramer (H4), composed of 4 Hla copies (in pink).

Table 1 Summary of the purification process for P4, P2H2 and H4^a

	P4	P2H2	H4
Purification step(s)	IMAC	IMAC (SEC)	IMAC, SEC
Purity	90%	81% (94%)	62%
Yield (per g of biomass)	7.2 mg	3.2 (2.0 mg)	0.7 mg

^a Abbreviations: IMAC, immobilized metal-ion affinity chromatography; SEC, size-exclusion chromatography.

method as opposed to chemical lysis, as it enabled recovery of most proteins in soluble form.

As the first purification step, all lysate supernatants were subjected to an immobilized metal-ion affinity chromatography (IMAC) binding the C-terminal His₆-tag and the His₃ spacers. In the case of P4, this first step was enough to yield a 90% purity, as determined through high performance liquid chromatography (HPLC) analysis (Fig. S2†). The high and effective full expression of PcrV compensated for the few PcrV-based impurities due to truncated forms of the full tetramer present after purification (Fig. S1†). However, in the case of P2H2, the presence of Hla reduced protein yields and introduced more impurities in the form of mono-, di- and trimers due to its less efficient expression. Therefore, a second purification step by size-exclusion chromatography (SEC) was needed, reaching 94% purity and decreasing the overall production yield. The third fusion protein, H4, gave the lowest yield and purity within the set of prepared tetramers. The H4 protein was also the least stable, requiring gentle manipulation as it was very prone to precipitation.

All chimeric protein tetramers were produced successfully, with the tetramer production comparable to that of the monomers. The expression of the hybrid PcrV and Hla dimer–dimer in particular (Fig. S1†) indicates that this strategy is suitable for multimeric fusion proteins. The P2H2 construct had production characteristics averaging those of the PcrV and Hla

proteins, suggesting a certain level of predictability for multimeric constructs of protein antigens with established expression and purification protocols.

The tetramers were subjected to a Western Blot (WB) analysis to ascertain the conservation of continuous protein epitopes (Fig. S3†). As expected, both P4 and H4 were recognized by their corresponding antibodies, and P2H2 was recognized by both anti-PcrV monoclonal antibodies (mAb) and anti-Hla serum. While only P4 and P2H2 could be obtained with a purity degree equal or superior to 90%, the purity standard for manufacturing²³ H4 was included in the study and used for the following conjugation.

Generation and derivatization of CP8 oligosaccharides

Conjugation of naturally sourced full-length polysaccharides is typically achieved in a random manner which can disrupt glycan epitopes as well as promote protein cross-linking and obstruction of key protein epitopes.⁴³ This also prevents from obtaining a clear association between immunogenicity and the conjugation site. To obtain a more defined glycoconjugate structure and minimize these challenges, shorter and more homogeneous CP8 oligosaccharides (OS) were generated to be random and site-selectively conjugated through their terminal end to the fusion proteins (Fig. 2). To this end, CP8 was hydrolyzed in acetic acid obtaining OS fragments with an average weight of 25 kDa, resulting from a distribution ranging from 5 to 50 kDa (Fig. S4†). Aminated intermediates were then produced by reductive amination at the reducing end of the OS by treatment with ammonium acetate in the presence of sodium cyanoborohydride (Fig. 2). To compare the His-tag-directed and the classic random conjugation, the aminated CP8 OS were derivatized with different linkers (Fig. 2). For the preparation of the site-selective conjugates, a dibenzylcyclooctyne (DBCO) moiety was introduced to be coupled to the azide moiety of a PEG₃-N₃ linker.³⁷ These were site-selectively attached to the histidine residues incorporated in the His₃



a) Reductive amination at the terminal end of CP8 oligosaccharides (OS)

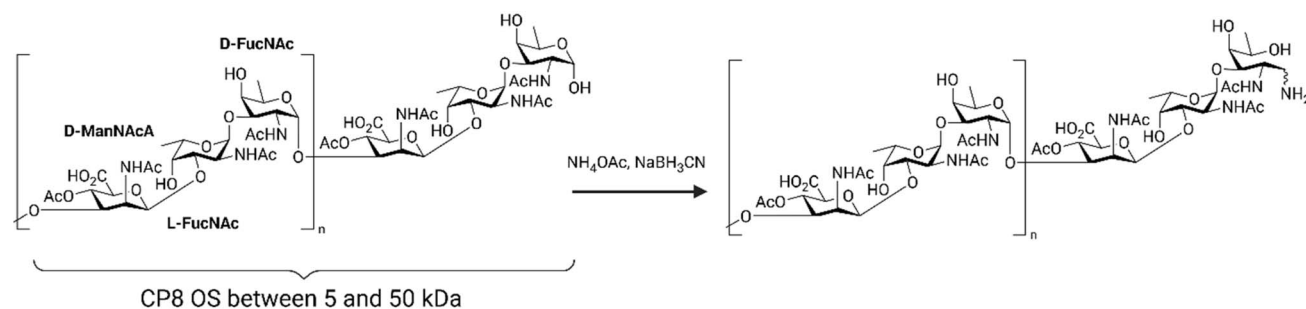
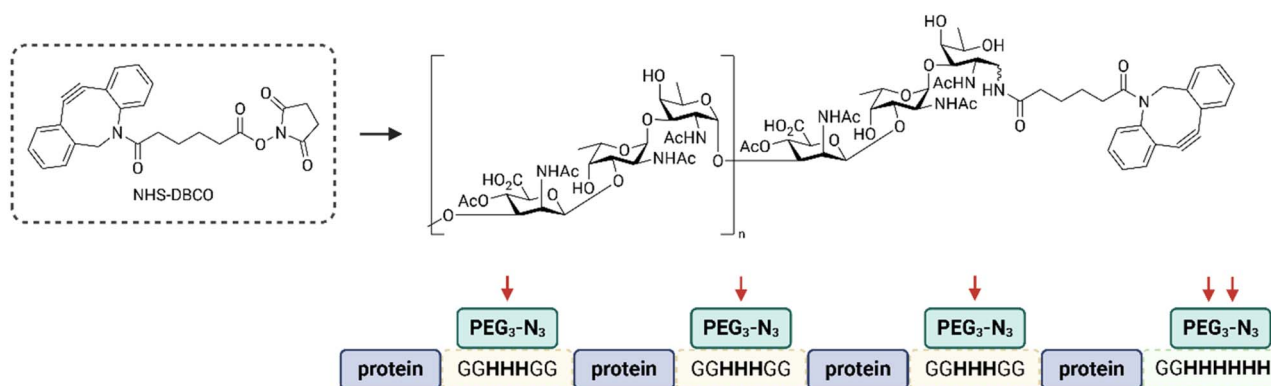
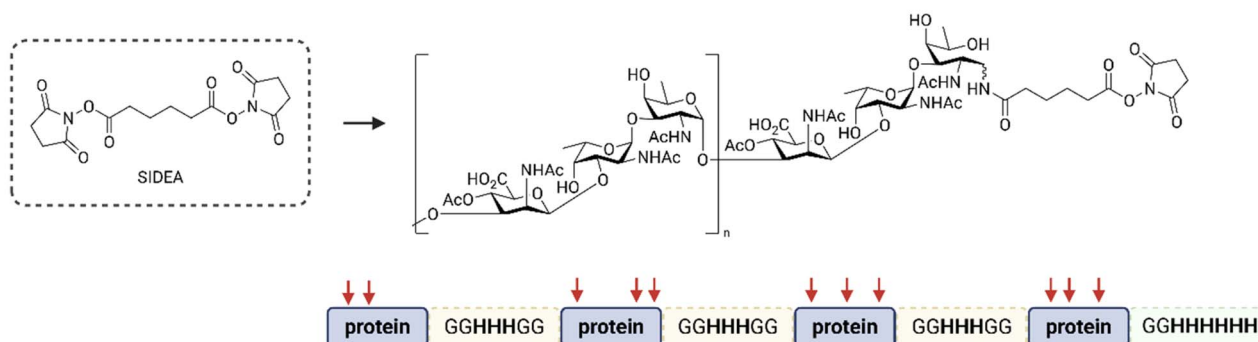
b) Derivatization of aminated CP8 OS for histidine tag-directed conjugationc) Derivatization of aminated CP8 OS for random conjugation

Fig. 2 Generation of CP8 oligosaccharides (OS) and derivatization strategies for the His-tag-directed and random conjugation, with different click-chemistries and corresponding coupling points indicated with the red arrows; (a) after hydrolysis of the polysaccharide, the generated CP8 OS were sized and reductively aminated at their terminal end with ammonium acetate; (b) aminated CP8 OS were derivatized with NHS-DBCO for site-selective glycoconjugation onto the carrier protein derivatized beforehand with bis-sulfone-PEG₃-N₃ on HxH motifs; (c) aminated CP8 OS were derivatized with SIDEA (di-(*N*-succinimidyl)adipate) directly onto the lysine residue sidechains of the carrier protein, corresponding to a traditional random glycoconjugation.

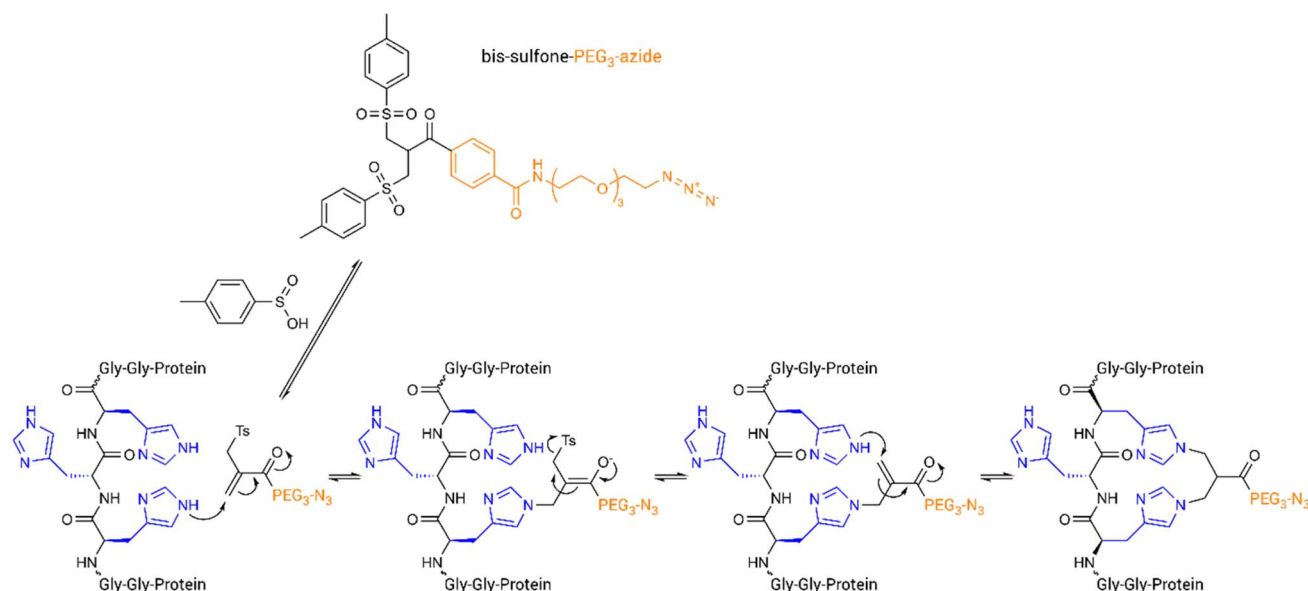
spacers between the protein copies and the C-terminal His₆-tag, through the use of a bis-sulfone reagent (Fig. 3). For the random conjugation strategy, the aminated OS were reacted with a bis(*N*-hydroxysuccinimide) (NHS) ester of adipic acid linker, to obtain an active ester ready for the subsequent reaction with the primary amine in the sidechain of the protein lysine residues.

Site-selective derivatization of the carrier proteins

For the site-selective glycoconjugates, the purified tetramers were first derivatized on the His₃ spacers and His₆-tag with a bis-sulfone-PEG₃-N₃ linker (Fig. 3). Bis-sulfone reagents can be used to bridge the imidazole rings of two nearby histidine residues in a protein by bis-alkylation (Fig. 3a). Bis-sulfones



a) Derivatization mechanism on HxH motifs



b) Carrier protein site-selective derivatization

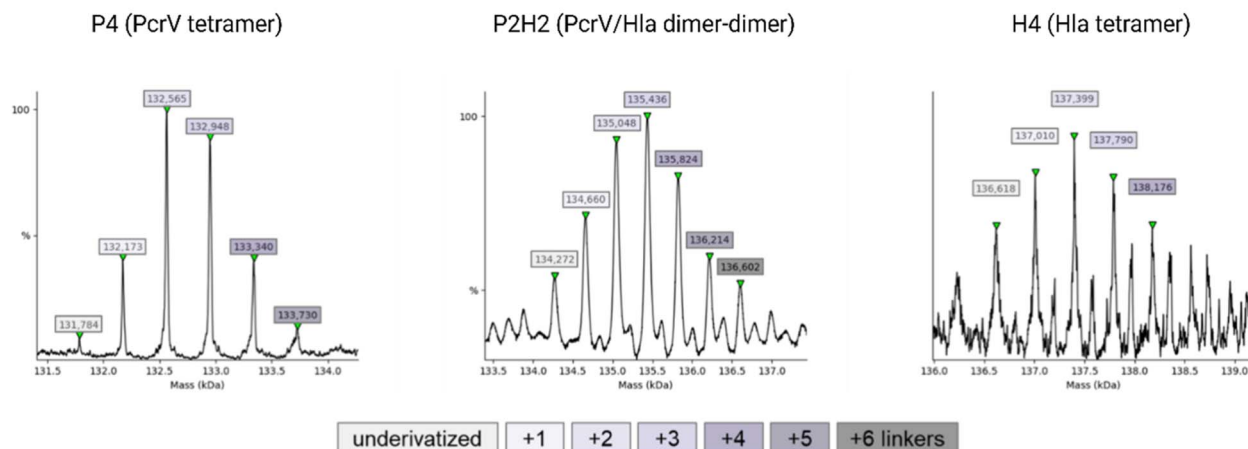


Fig. 3 Site-selective derivatization of the carrier protein on HxH motifs (a) proposed derivatization mechanism: the linker is first equilibrated for 6 h at 37 °C in a 7 : 3 mixture of dimethyl sulfoxide (DMSO) and buffer (15 mM sodium phosphate, 1.5 mM ethylenediaminetetraacetic acid (EDTA), pH 5.0) to yield the reactive mono-sulfone after elimination of *p*-toluenesulfonic acid; the protein is then bis-alkylated at the imidazoles of spatially close histidine residues (in blue) by a sequence of addition–elimination reactions on the GGHHHG (His₃) spacers and the His₅-tag inserted in the tetramers; (b) ESI-MS spectra from derivatized P4 (left), with 5 equivalents of bis-sulfone-PEG₃-N₃ linker, at 30% DMSO (underivatized peak at 131.784 kDa); P2H2 (center), with 8 equivalents of linker, without DMSO (underivatized peak at 134.272 kDa); H4 (right), with 10 equivalents of linker, without DMSO (underivatized peak at 136.618 kDa); all reactions were conducted at pH 5.0 in 50 mM sodium acetate for 25 h at room temperature (rt).

equilibrate to mono-sulfones, which can then engage in an addition–elimination mechanism relying on the Michael reaction and achieve a site-specific protein functionalization. Due to their lower pK_a compared to other nucleophilic residues, such as lysine and arginine, histidines remain unprotonated and reactive at mildly acidic pH (5–6), making derivatization of lysine residues less favorable under these conditions.³⁷ Notably, this reaction can target native disulfide bonds in proteins,⁴⁴ though these are absent in Hla and PcrV. Based on the design of

the carrier proteins, it was expected that up to 6 linkers could be added to the HxH motifs, although derivatization of lysine residues and/or other spatially close histidine residues could result in the attachment of additional copies of the linker. Due to its phenyl groups, the bis-sulfone-PEG₃-N₃ is a poorly water-soluble compound and to solubilize a sufficient amount of the linker reagent, dimethyl sulfoxide (DMSO) was used as a cosolvent. The functionalized proteins were analyzed using electrospray ionization (ESI)-mass spectrometry (MS) to evaluate the



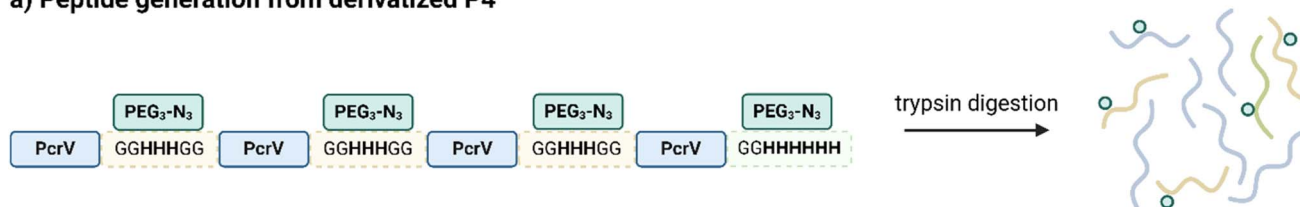
derivatization level of the proteins (Fig. 3b), and nano-differential scanning fluorimetry (nanoDSF) was used to exclude protein aggregation and loss of yield (Fig. S5†).

Incorporation of up to 5 linkers could be observed for P4 (133.730 kDa), with the majority of P4 carrying 2 or 3 linkers (132.565 and 132.948 kDa, respectively). For P2H2, the addition of up to 6 linkers (136.602 kDa) was detected; however, similarly to P4, an average incorporation of 2 and 3 molecules was achieved (135.048 and 135.436 kDa, respectively). Derivatization of H4 was slightly less effective, with MS analysis showing mostly the addition of only 2 linkers (137.399 kDa).

The site-selectivity of the reaction was investigated through ESI-MS mapping of peptides derived from trypsin digestion of both underivatized and derivatized P4 samples (Fig. 4a). The selective digestion ensured the production of identical peptides from both derivatized and underivatized proteins, which minimized the risk of generating non-comparable peptides due to the derivatization process. Attached linkers could interfere with a random digestion (*e.g.* with pepsin) and complicate the

peptide comparison. Addition of the azide linker (+388 Da) was observed in peptides with a MW corresponding to the His₃ spacers, the His₆-tag and to an internal PcrV peptide with one histidine and one lysine residue (Fig. 4b and S6†). While it was not possible to determine whether the linker in the latter peptide was attached through one or two arms of the linker (Fig. 3a), the linker was assumed to be connected through only the histidine residue, as trypsin cleaves at the C-terminus of lysine residues, and a derivatization at the side-chain would prevent cleavage after a functionalized residue.^{45,46} Notably, the C-terminal His₆-tag peptide only carried one derivatization, and no double derivatization was identified despite the six consecutive histidine residues. While the generated peptides were not quantified, the three identified modifications can account for all the observed functionalization in the fusion proteins. There is, however, the possibility of other modifications, such as the derivatization of peptides with non-contiguous histidine residues, which would bridge two spatially close but distinct regions of the protein. This latter modification would not be

a) Peptide generation from derivatized P4



b) Identification of derivatized peptides

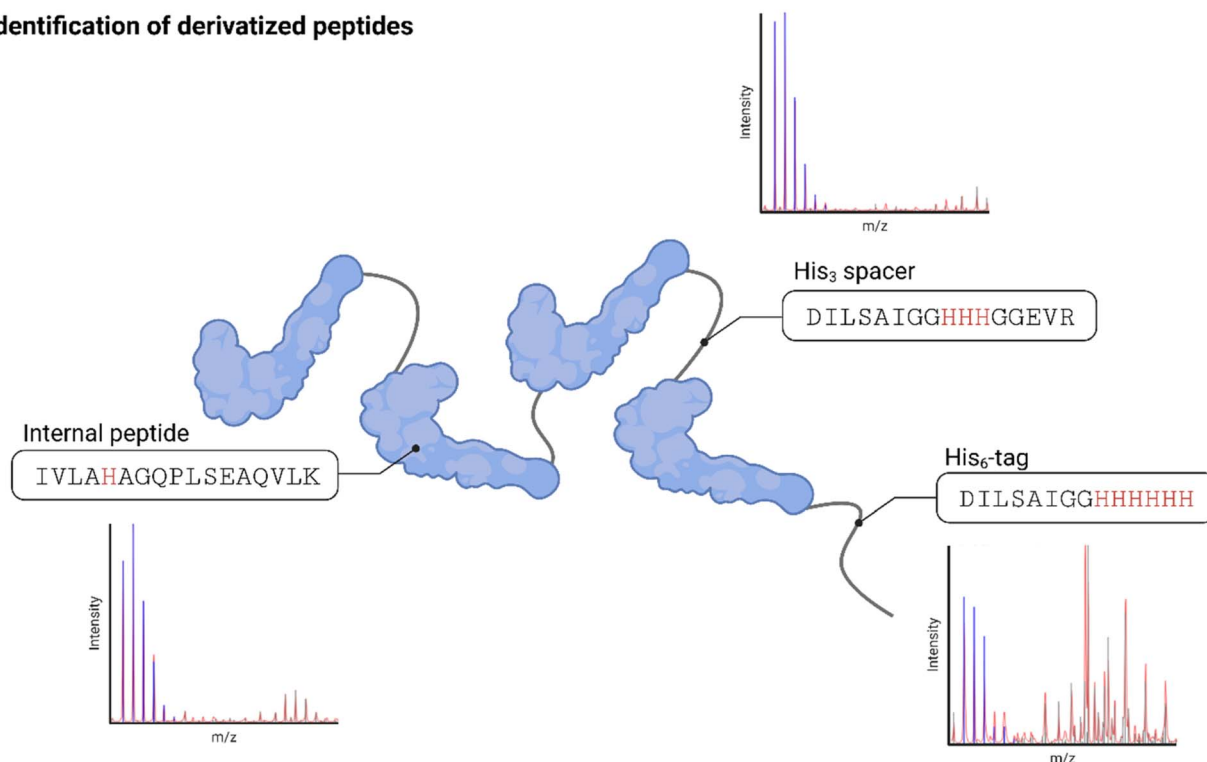


Fig. 4 Schematic representation of the peptide mapping for a derivatized P4 sample to confirm the site-selectivity of the conjugation chemistry on histidine residues; (a) derivatized P4 was fragmented into peptides enzymatically by trypsin; (b) derivatized peptides were analyzed in ESI-MS against an underivatized reference (ESI, Fig. 6†) and three derivatization sites were confirmed.



detectable by the software using this technique, as it relies on the primary sequence of the protein. Notably, no peptides were found where lysine residues were functionalized with a linker.

The same analysis on P2H2 revealed similar results, with only traces of the functionalized internal peptide from PcrV (data not shown). The derivatization behaved therefore similarly with another protein, and no functionalized internal peptide was found in Hla, indicating that off-site functionalization, like that observed with the internal PcrV peptide, is likely a rare occurrence.

Taking together these data, all the modified proteins were primarily derivatized with a single linker at the purposely introduced histidine motifs, while modifications of other amino acid residues, such as lysine, were ruled out.

Generation and immunization of the glycoconjugates

Once the site-selectivity of the derivatization of the carrier proteins on His₃ spacers and His₆-tag was confirmed, all conjugate vaccines were produced. Both site-selective and random conjugates with CP8 OS were generated for all tetramers, to compare the effect of the two conjugation chemistries on the immunogenicity of the conjugates. To evaluate the benefits of a tetrameric construct over a monomeric one, a random conjugate of a wild-type PcrV monomer (PcrV_{wt}) to CP8 OS was also prepared. The final conjugates' production summary can be found in Table 2. The residual free protein and free saccharide were evaluated by sodium dodecyl sulfate-








polyacrylamide gel electrophoresis (SDS-PAGE, Fig. S7†) and by HPLC, respectively, and the integrity of the proteins was assessed by WB (Fig. S8†). The random and site-selective conjugation chemistries resulted in considerable differences in saccharide loading (Table 2). Generally, random conjugates had a saccharide-to-protein weight ratio around 10 times higher than their site-selective counterparts, with the exception of P2H2, which showed similar ratios for both conjugation methods (0.7 and 0.9 w/w, respectively). Given the limited number of lysine residues in the protein monomers (16 and 28 for PcrV and Hla monomers, respectively), as well as the similar w/w ratios for the random PcrV-based conjugates and the random H4 conjugate, it was estimated that all the available lysine residues were most likely glycoconjugated in the random conjugates.

To evaluate the vaccine potential of the new glycoconjugate *in vivo*, groups of eight CD1 mice were immunized on days 1 and 22 *via* intramuscular injection with 1 µg, based on saccharide content, of each multimeric construct. As controls, CP8 conjugates with monomeric protein PcrV_{wt} and the CRM₁₉₇ carrier, commonly used in licensed vaccines, were used. Because the vaccine dosage was based on the saccharide content, resulting in varying amounts of proteins in the diverse glycoconjugates (Table S2†), two different dosages of the monomeric proteins PcrV_{wt} and Hla_{H35L} were chosen for comparison to closely match the protein amounts in the corresponding multimeric conjugates. Specifically, a dosage of approximately 5 µg was used to match the protein content of the P4 and H4 site-selective conjugates. For the P4, PcrV_{wt}, and H4 random conjugates, as well as the random and His-directed P2H2 conjugates, the control protein dosage was set at 0.5 µg, reflecting the average protein content delivered by the conjugates.

All vaccines elicited an anti-CP8 response comparable to the CRM₁₉₇ benchmark, except the P4 and PcrV_{wt} random conjugates (Fig. 5a). This consistent response across the conjugates was achieved despite varying CP8 OS loadings, including the site-selective conjugates having a lower saccharide content (Fig. 3b and Table 2). PcrV appeared as a weak carrier compared to Hla_{H35L} and CRM₁₉₇, leading to lower anti-CP8 antibody levels. Both the site-selective and the random P4 conjugates failed to elicit a stronger immune response than the CRM₁₉₇ control, indicating that neither the additional copies nor the multimeric presentation improved the carrier effect. However, the P4 site-selective conjugate showed a significantly stronger response than the P4 random conjugate, which gave a poor immune response, similar to the monomeric PcrV_{wt} random conjugate.

As opposed to the P4 conjugates, both the random and the site-selective P2H2 conjugates performed well in terms of anti-CP8 response, with significantly higher titers than P4. This suggests that the presence of the two Hla copies compensated for PcrV's limited ability as a protein carrier. Despite random conjugates generally carrying more saccharide moieties than their site-selective counterparts (Table 2), anti-carbohydrate immune responses were not statistically different between the random and the His-directed conjugates. In particular, the H4

Table 2 High-performance anion-exchange chromatography with pulsed amperometric detection (HPAEC-PAD) analysis of the saccharide content of the CP8 conjugates generated with various protein carriers

		Saccharide/protein (w/w)
	P4-CP8 site-selective	0.2
	P4-CP8 random	2.2
	PcrV _{wt} -CP8 random	4
	P2H2-CP8 site-selective	0.7
	P2H2-CP8 random	0.9
	H4-CP8 site-selective	0.2
	H4-CP8 random	1.9

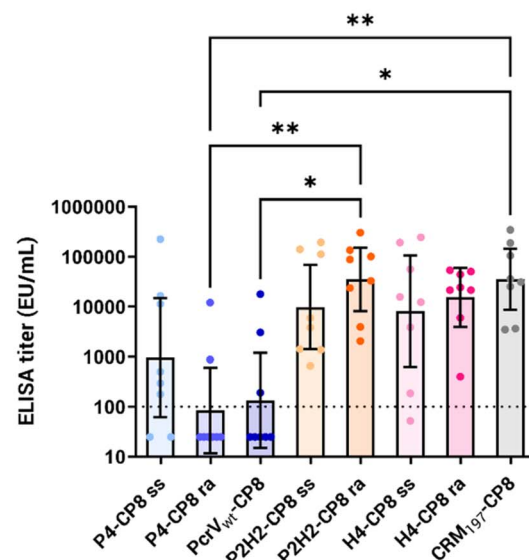


a) Amount [μg] of each antigen per injection

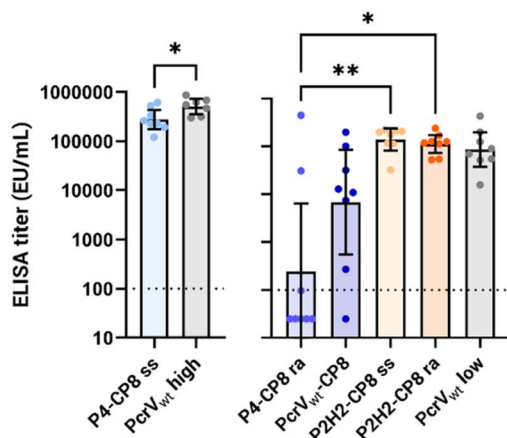
Glycoconjugate vaccines							
	P4-CP8		PcrV _{wt} -CP8	P2H2-CP8		H4-CP8	
	ss	ra		ss	ra	ss	ra
CP8	1	1	1	1	1	1	1
PcrV	5	0.5	0.3	0.6	0.5	-	-
Hla	-	-	-	0.6	0.5	5	0.5

Control proteins			
	PcrV		Hla
	high	low	
CP8	-	-	-
PcrV	5	0.5	-
Hla	-	-	5

b) Anti-CP8 IgG titers



c) Anti-PcrV IgG titers



d) Anti-Hla IgG titers

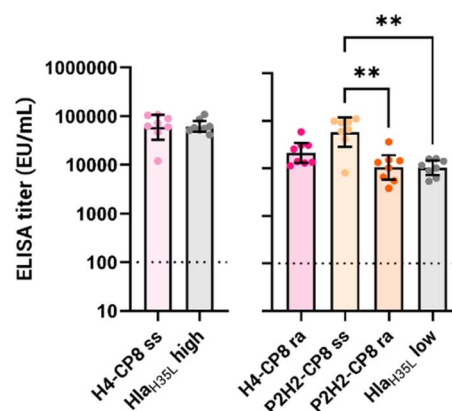


Fig. 5 Immunological evaluation of the generated vaccines. (a) Summary of the injected amounts [μg] for each antigen included in the glycoconjugate vaccines. PcrV_{wt} and Hla_{H35L} were administered either as a 5 μg injection, equivalent to the average protein content in the site-selective P4 and H4 conjugates, or as a 0.5 μg injection, equivalent to the protein content in the random P4 and H4 conjugates and half of the P2H2 conjugate injections. Enzyme-linked immunosorbent assay (ELISA) immunoglobulin G (IgG) titers (b) anti-CP8, (c) anti-PcrV and (d) anti-Hla in mouse serum samples collected after 2 vaccine doses (EU mL^{-1} , arbitrary units). For clarity, anti-PcrV and anti-Hla titers are shown alongside their corresponding control monomeric protein injection (in grey). Bars represent the geometric mean titers with 95% confidence intervals from 8 serum samples; $p^* < 0.05$ and $p^{**} < 0.002$ (Kruskal–Wallis and Dunn's test for multiple comparison, Mann–Whitney's test for single comparison). The dotted line at 100 EU mL^{-1} represents the detection limit of the assay, under which the titer is considered negative. Abbreviations: IgG, immunoglobulin G; ra, random conjugate; ss, site-selective conjugate.

site-selective conjugate showed a more scattered response than its random counterpart, although the difference was not statistically meaningful. Notably, the H4 site-selective conjugate had nearly 10 times lower saccharide loading than the H4 random conjugate (Table 2), suggesting that higher saccharide loading might help ensuring a more robust immune response. However, in the case of P2H2, where both random and His-directed conjugates bore a similar amount of glycan (0.9 and 0.7 w/w, respectively), the anti-CP8 antibody levels were clearly statistically comparable.

Overall, the site-selective conjugates achieved similar responses to the random ones, despite their lower carbohydrate loading (Fig. 3b), indicating that one attachment site was sufficient to provide a robust carbohydrate specific immune response with the CP8 OS length used.

Looking at the anti-PcrV responses, the P4 site-selective conjugate provided a more robust protein-specific response (Fig. 5b) compared to the P4 and PcrV_{wt} random conjugates, which yielded significantly lower titers. Two factors could explain this result. First, at the administered CP8 dose, the P4 site-selective conjugate had approximately 10 times more



protein than its random counterpart. On the other hand, it should be considered that nearly all lysine residues of P4 and PcrV were engaged by the random conjugation, likely compromising the protein's integrity. Importantly, both the P2H2 random and site-selective conjugates elicited similar anti-protein antibody responses while having a similar glycan and protein content ($\sim 0.5 \mu\text{g}$ at the tested CP8 dose), exceeding those achieved with the P4 random conjugate. On the whole, these findings suggest that PcrV alone is not an optimal carrier for glycoconjugate vaccines. However, fusing multiple copies of the same protein or combining it with Hla improves its carrier properties. In addition, directing the conjugation to specific sites can help preserve the protein structure and prevent the disruption of immunogenic protein epitopes.

Turning attention to the staphylococcal toxin, all Hla_{H35L}-based conjugates elicited strong responses against Hla (Fig. 5c), comparable to those induced by the monomeric Hla_{H35L}. As opposed to the anti-PcrV response, the P2H2 site-selective conjugate generated a noticeably superior response against Hla compared to the randomly conjugated version as well as the control Hla_{H35L}. This improved response against Hla, which was not achieved by the H4 and P2H2 random conjugates of similar size, highlights the role of site-selective conjugation in enhancing the Hla-specific immune response, rather than the presence of a fused protein.

Combining the immune responses against PcrV, Hla and CP8, the P2H2 site-selective construct emerged as the lead vaccine candidate, generating a strong response against all three antigens. The strong responses elicited by the His-directed conjugates, particularly P2H2, against both protein antigens (Fig. 5b and c) highlighted the advantage of the site-selective chemistry for preserving critical protein epitopes, which is an important feature for proteins with the dual role of antigen and carrier. Furthermore, the fusion of Hla to PcrV was an impactful strategy to enhance the carrier properties of PcrV and achieved enhanced anti-CP8 immune responses compared to the PcrV monomer.

Next, the functional activity of anti-Hla antibodies was evaluated in a hemolysis inhibition assay, in which the capacity of the pooled mice sera to protect rabbit erythrocytes from the toxic activity of Hla wild-type (Hla_{wt}) was assessed (Table 3). All sera obtained from two injections of the Hla-based conjugates demonstrated a neutralization capacity against Hla_{wt}, equivalent to the controls.

The site-selective and random P2H2 conjugates exhibited a neutralization titer of 383 and 336, respectively, which slightly outperformed the control protein (254), possibly due to the presence of two Hla copies, leading to different uptake and antigen processing, or to an adjuvant effect^{19,47} from the carbohydrate. Importantly, the H4 site-selective conjugate showed the highest neutralization titer in the set (1031) which was higher than its random counterpart (605). Also, the His-directed and random H4 conjugates gave a remarkably stronger functional response than the Hla_{H35L} monomer administered at the corresponding protein dosages (738 and 247, respectively). Given that H4 contains four copies of Hla_{H35L}, this suggests that the number of protein copies, *i.e.* the

Table 3 Neutralizing titers of the sera elicited towards the different conjugates measured against Hla_{wt}^a

		Sera neutralizing titers	
		Post 1	Post 2
Equivalence 1	H4-CP8 site-selective conjugate	80	1031
	Hla _{H35L} 5 μg	Negative	738
Equivalence 2	H4-CP8 random conjugate	Negative	605
	P2H2-CP8 site-selective conjugate	Negative	383
	P2H2-CP8 random conjugate	Negative	336
	Hla _{H35L} 0.5 μg	Negative	247

^a For clarity, the titers were separated by comparable protein injections: Hla_{H35L} 5 μg is a monomeric protein injection equivalent to the average protein content for the site-selective H4 conjugate; Hla_{H35L} 0.5 μg is equivalent to the protein content for the random H4 conjugate and half of the P2H2 conjugate injections. The neutralization titer (IC₅₀) is defined as the serum dilution giving 50% inhibition of hemolysis.

multivalency of the construct, rather than the presence of CP8 is responsible for the increased antibody functionality. Additionally, the neutralizing titers of the site-selective conjugates generally exceeded those of their random counterparts, with the H4 site-selective conjugate showing a functional response (80) even after one dose (Fig. 5a and S9†). These data align with the measured antibody levels (Fig. 5c), corroborating the site-selective conjugation chemistry as a more suitable approach to preserve the Hla protein structure.

Altogether, the immune responses elicited by the PcrV- and Hla-based conjugates suggest that combining protein antigens can enhance the immune response against each respective antigen. These results support the overall hypothesis that carefully crafted conjugates can preserve critical epitopes, achieving a synergistic combination of protein and carbohydrate antigens.

Conclusion

In this work, multimeric fusion proteins were used to compare a classic random conjugation strategy at lysine residues with the site-selective conjugation of spatially close histidine residues. Chimeric protein tetramers were successfully produced with yields comparable to monomers. A histidine-tag-directed derivatization proved to be a viable method for glycoconjugation, effectively preserving protein integrity and enhancing immune responses.

In terms of antibody levels, the P4 site-selective conjugate induced a stronger response than its random counterpart, likely due to the better preservation of protein epitopes. Most vaccines, except for the random PcrV-based conjugates, performed comparably to the CRM₁₉₇ conjugate benchmark in eliciting a response against CP8. Notably, the histidine-tag-directed P2H2 conjugate showed a robust immune response against all three antigens, CP8, PcrV and Hla.

The use of fusion proteins to generate multivalent carrier proteins, paired with site-selective chemistry, shows promise for developing multipathogen vaccines. Fusion proteins



performed as well as established carriers like CRM₁₉₇, and in the case of P2H2, each antigen contributed to enhancing the overall immune response. The multivalency of chimeric proteins appears to offer an advantage over simply combining antigens into a single formulation, as indicated by the slight increase in antibody functionality observed with multivalent Hla carriers. Additionally, fusion proteins enable the synergistic combination of antigens, potentially boosting antibody titers, as suggested by the presence of PcrV enhancing the response against Hla in the P2H2 site-selective conjugate.

Histidine-directed conjugation emerges as a versatile method for coupling carbohydrates to proteins, offering advantages over other techniques such as bioconjugation in accommodating a wide range of saccharides, from synthetic oligosaccharides to full-length polysaccharides, and allowing fine control of the sugar-to-protein ratio. Although in the present work, achieving a high saccharide loading in the site-selective conjugates was not evaluated, incorporation of additional HxH motifs can be envisaged to increase the number of carbohydrate moieties attached.

Overall, the findings from this work on protein carrier design and conjugation strategies may be valuable in the development of future glycoconjugate vaccines aimed at targeting simultaneously multiple pathogens.

Materials and methods

Production and characterization of the chimeric protein carriers

All three designed plasmids corresponding to P4, P2H2 and H4 were synthesized by GeneArt (Thermo Fisher). The tetramer sequences were cloned into a pET303-CT vector including a His₆-tag at the C-terminal.

P4 was expressed in BL21 Star (DE3) cells, while P2H2 and H4 were expressed in BL21 (DE3) cells (Fig. S1†). The cells were first grown at 37 °C for 8 h in lysogeny broth (LB) medium supplemented with 100 mg L⁻¹ of ampicillin, and then transferred by a 1:100 dilution into HMC medium (glycerol 15 g L⁻¹, yeast extract 30 g L⁻¹, MgSO₄ 0.5 g L⁻¹, KH₂PO₄ 5 g L⁻¹, K₂HPO₄ 20 g L⁻¹, KOH 1 M; pH 7.3) with a 24 h induction (1 mM IPTG) at 20 °C, 160 rpm. To improve H4 expression, induction trials at different timepoints were performed, and H4 expression was ultimately induced for 6 h at 20 °C, 160 rpm, to reduce the amount of Hla-based impurities. Cells were harvested and pelleted by centrifugation at 12 000 g, at 4 °C for 30 min. Cell pellets were resuspended in lysis buffer (30 mM Tris, pH 8.0, 0.25 mg mL⁻¹ lysozyme, 1 mM MgCl₂, 10 U benzonase, supplemented with EDTA-free complete Protease Inhibitor Cocktail; Roche) and lysed, either chemically for P4 through addition of the B-PER Bacterial Protein Extraction Reagent (Thermo Scientific), or mechanically through sonication for P2H2 and H4 (40% amplitude, with alternating pulse and rest cycles of 30 s on ice).

Lysis supernatants were collected by centrifugation at 12 000 g, at 4 °C for 30 min, and then purified by Co²⁺ affinity (HiTrap TALON crude; Cytiva) in a single-step elution in purification buffer (50 mM sodium phosphate, pH 8.0, 300 mM NaCl) with a gradient up to 250 mM imidazole. The collected

and pooled fractions were concentrated in Phosphate Buffered Saline (PBS) buffer through Vivaspin® 15, 10 kDa MWCO, Centrifugal Concentrators (Sartorius). In the case of H4, the protein was subjected to an additional size-exclusion chromatography (SEC, Sephacryl S-200 HR; Cytiva) in PBS.

Protein concentrations were determined through bicinchoninic acid (BCA) assay against a bovine serum albumin (BSA) standard curve using the Pierce BCA Protein Assay Kit (Thermo Fisher).

The purified proteins were analyzed by SDS-PAGE and subsequently by WB (Fig. S3†). Gels were run using 4 to 12% Bis-Tris protein Gel NuPAGE, 4–12%, Bis-Tris, 1.0 mm, Mini Protein Gel, 12-well gels in morpholineethanesulfonic acid (MES) SDS running buffer (NuPAGE; Invitrogen). Proteins were transferred onto nitrocellulose membranes (0.2 µm pore size; NuPAGE; Invitrogen) for 7 min at 20–25 V using an iBlot module (Invitrogen). The membrane was blocked with 3% BSA in PBS overnight at 4 °C, then washed three times with PBS, supplemented with 0.05% Tween 20, and incubated for 1 h with anti-Hla serum or anti-PcrV mAb. The membrane was then washed again as described above and incubated for 1 hour with alkaline phosphatase (AP)-conjugated anti-mouse IgG (Sigma-Aldrich) diluted 1:1000 in blocking buffer. The membrane was finally washed three times and binding was detected using the colorimetric AP substrate reagent kit (Bio-Rad).

Site-selective derivatization of the chimeric protein carriers

The bis-sulfone-PEG₃-N₃ linker (BroadPharm) was pre-incubated 6 h at 37 °C at a concentration of 2 mg mL⁻¹, in a solution of 70% dimethyl sulfoxide (DMSO) and 30% buffer (15 mM sodium phosphate, 1.5 mM ethylenediaminetetraacetic acid (EDTA), pH 5.0) to yield the reactive mono-sulfone.

The protein derivatization reaction was carried out for 25 h at rt in 50 mM sodium acetate buffer at pH 5.0. The pH was an important parameter to keep below the pK_a of lysine residues, to ensure the selectivity on histidine. Different conditions for all tetramers were explored, reflecting their different behavior. P4 was incubated with 5 equivalents of linker in 30% DMSO, while P2H2 and H4 reacted with 8 and 10 equivalents of linker, respectively, in the absence of added DMSO. The derivatized proteins were purified twice through Zeba™ Spin Desalting Columns, 7 K MWCO, 0.5 mL (Thermo Scientific) in PBS.

The impact of the added 30% DMSO after 26 h was evaluated on P4 through nano differential scanning fluorimetry (Tycho, NanoTemper) and found to be acceptable (Fig. S5†).

Generation and derivatization of the CP8 oligosaccharides

Isolated and purified CP8 was hydrolyzed in acetic acid 2% for 16 h, at 90 °C to OS of a MW ranging from 5 to 50 kDa, with an average of 35 kDa (depending on the CP8 batch, additional hydrolysis time was required, Fig. S4†). The reaction was neutralized with NaOH 2 M, the OS desalted in water through a 124 mL desalting column (Sephadex G-25; Cytiva) and lyophilized. The dry hydrolyzed OS were resuspended and sized through anion-exchange chromatography (HiTrap Q FF column 5 mL; Cytiva). Pools were analyzed by HPLC (TSK G3000PWXL;



Tosoh Bioscience) against a range of pullulans, and merged for CP8 OS weighing between 5 and 50 kDa.

The sized CP8 OS were desalted again in water, lyophilized and resuspended in sodium acetate 150 mM, pH 7.0. The fragments were then aminated at their reducing end through reductive amination, with ammonium acetate (300 mg mL⁻¹, added as a solid) and sodium cyanoborohydride (49 mg mL⁻¹ solubilized in sodium acetate 150 mM, pH 7.0) at an approximate 3 mg mL⁻¹ concentration of OS. The reaction was left for 4 days at 37 °C.

The aminated CP8 OS were first purified in NaCl 200 mM, and then desalted in water through a 124 mL desalting column (Sephadex G-25; Cytiva). Primary amines were quantified through colorimetric assay against a standard curve of 6-aminoacaproic acid. From there, two different OS derivatizations were performed depending on the conjugation strategy intended.

For the site-selective conjugation strategy, a dibenzylcyclooctyne (DBCO)-*N*-hydroxysuccinimide (NHS) ester linker was introduced at the aminated end of the OS, to be coupled to the azide (N₃) moiety of a bis-sulfone-PEG₃-N₃ linker, site-selectively attached to the carrier protein beforehand. The aminated CP8 OS were solubilized in a 9 : 1 DMSO : H₂O solution, to which 10 equiv. of linker and 5 equiv. of triethylamine were added. The reaction was left for 3 h at rt, desalted in water, lyophilized and analyzed by NMR to confirm the presence of DBCO.

For the random conjugation strategy, another bifunctional linker, the adipic acid bis(NHS ester), was inserted at the OS terminal amine, for subsequent reaction with the amine of the lysine residues' sidechains. The aminated CP8 OS were solubilized in a 9 : 1 DMSO : H₂O solution, to which 10 equiv. of linker were added. The reaction was left for 2 h at rt, and purified by precipitation in 5 mL cold ethyl acetate, to which 250 µL of NaCl 3 M were added to favor OS precipitation. The solution was left for 1 h at 4 °C then centrifuged, the supernatant removed and the bottom phase washed with cold ethyl acetate. The OS were washed until a white precipitate was formed, which was lyophilized.

Site-selectivity analysis by mass spectrometry

P4 and P2H2 were selectively digested and analyzed by ESI-MS in both their underivatized and derivatized forms with the bis-sulfone-PEG₃-N₃ linker. Trypsin (Sequencing Grade, modified from porcine pancreas; Serva), targeting arginine and lysine residues, was used for digestion. Protein samples were denatured at 95 °C for 5 minutes before digestion in PBS at a protein-to-trypsin ratio of 0.04 (w/w) for 3 hours at 37 °C.

Post-digestion, reversed-phase purification was performed using Oasis® HLB 30 µm sorbent cartridges (Waters). The cartridges were prepped per the manufacturer's instructions: 400 µL acetonitrile for activation, followed by equilibration with 600 µL of 0.1% aqueous formic acid thrice. Samples, acidified with 40 µL of 1% formic acid, were loaded and passed through the column multiple times for optimal peptide retention. The column was washed with 600 µL of 0.1% aqueous formic acid thrice to remove impurities. Peptides were eluted with 300 µL of 60% acetonitrile in 1% formic acid water twice, then concentrated and stored after solvent removal.

Peptides were injected at 200 µL min⁻¹ in 100% buffer A (0.23% formic acid in water). Separation occurred through an ACQUITY UPLC® HSS T3 reverse phase column (1.8 µm, 1.0 × 100 mm; Waters) with a gradient from 10% to 40% buffer B (0.23% formic acid in acetonitrile) over 6.8 minutes at 40 µL min⁻¹.

The peptides were then infused into a SYNAPT G2-Si mass spectrometer (Waters) with a standard ESI source, calibrated with a 100 fmol µL⁻¹ [Glu1]-fibrinopeptide solution. Data acquisition was performed in MSE resolution mode (300–2000 *m/z* range, 0.3 s scan time, 0.1 s interscan time, 4.0 eV trap collision energy, 2 eV transfer collision energy, 25 V cone voltage, 90 °C source temperature, 3000 V capillary voltage). Argon was used as the collision gas, with mass accuracy maintained by continuous Glu-Fib infusion at 5 µL min⁻¹.

Peptides were identified using Protein Lynx Global Server 2.5 (Waters) and further verified with DynamX V 3.0 software (Waters). Selection criteria included peptides present in at least 4 of 5 replicates, <10 ppm mass error, and a minimum of 0.2 identified peptides per amino acid residue. Manual inspection was conducted to eliminate false identifications. Labeled peptides were analyzed and aligned using DynamX, followed by manual curation to ensure correct isotope alignment and assignment.

Conjugation and characterization of the glycoconjugates

For site-selective conjugation, CP8 OS-DBCO samples were lyophilized and resuspended into concentrated derivatized tetramers in a theoretical 1 : 1 protein : OS ratio (as calculated with a theoretical OS concentration). For random conjugation, CP8 OS-SIDEA corresponding to 15 equivalents was weighed and resuspended into concentrated tetramers. The reactions were left overnight at 4 °C and purified through SEC (Sephacryl S-200 HR, Cytiva) in PBS for conjugates P4-CP8 random, P2H2-CP8 site-selective and random, P4-CP8 site-selective and random. The P4-CP8 site-selective conjugate was purified in PBS through ultracentrifugation (Vivaspin 0.5 mL, 50 K MWCO; Sartorius) at 4500 g (10 min cycles), however, protein recovery was suboptimal and SEC was chosen for the next conjugate. The conjugate was washed 30 times with 100 µL PBS1x. All conjugates were filtered sterile through 0.22 µm and the protein content was quantified by BCA assay.

Gels were run to confirm the minimal residual free protein using NuPAGE, 3–8%, Tris-acetate, 1.0 mm, Mini Protein Gel, 12-well gels in Tris-acetate SDS running buffer (NuPAGE; Invitrogen) (Fig. S7†).

The quantification of saccharide was performed by HPAEC-PAD analysis using standard samples of CP8 at seven increasing concentrations, ranging between 0.1 and 3.0 µg mL⁻¹, to build the calibration curve. The reference and analytical samples were incubated at 100 °C for 3 hours in 4 M HCl, dried under vacuum (SpeedVac, Thermo), suspended in water and filtered with 0.45 µm Phenex-NY (Phenomenex) filters. The HPAEC-PAD analysis was performed in a Dionex ICS-6000 equipped with a CarboPac PA1 column (4 × 250 mm; Dionex) coupled with a PA1 guard to column (4 × 50 mm; Dionex) using isocratic elution in 16 mM NaOH.



Bacterial endotoxin levels were quantified through Limulus ameocyte lysate (LAL) assay using an Endosafe PTS spectrophotometer (Charles River) and found acceptable for immunization.

Mice immunization and sera analysis

Animal studies were conducted according to experimental guidelines from the Animal Welfare Body of the Animal Resource Centre at GSK.

Groups of eight CD1 mice were immunized on days 1 and 22 by intramuscular injection of 1 μ g (saccharide-based) of each glycoconjugate or 0.5/5 μ g of monomeric control proteins, adsorbed on alum hydroxide adjuvant. Sera were bled at days 0 (pre-immunization), 21 (blood sample) and 42 (final bleed). IgG titers in collected sera were estimated by ELISA. 96-well microtiter plates were coated with 100 ng of CP8 polysaccharide. Plates were incubated overnight at 4 °C, washed three times with PBST (0.05% Tween-20 in PBS pH 7.4) and saturated with 250 μ L per well of blocking buffer (3% bovine serum albumin in PBST) for 90 min at 37 °C. Two-fold serial dilutions of sera in blocking buffer were added to each well. Plates were then incubated at 37 °C for 1 h, washed with PBST, and then incubated for 90 min at 37 °C with anti-mouse (whole molecule) IgG-alkaline phosphatase (Sigma-Aldrich) diluted 1 : 2000 in blocking buffer. The plates were washed and developed with a 4 mg mL⁻¹ solution of *p*-nitrophenyl phosphate (pNPP) in 1 M diethanolamine (DEA) pH 9.8, at rt for 30 min. The absorbance was measured using a SPECTRAMax plate reader 405 nm. IgG titers were calculated by the reciprocal serum dilution giving an Optical Density (OD) of 1.

Neutralization activity of anti-Hla antibodies was evaluated by hemolysis inhibition assay. Briefly, serial two-fold dilutions of serum (1 : 50 first dilution point) containing anti-Hla antibodies were incubated with native α -hemolysin (Hla_{wt}) to allow the immunocomplex formation. Rabbit erythrocytes (RBC) were then added and lysed with residual free toxin. Hemolysis was evaluated by measuring the absorbance of the reaction supernatant at $A_{405\text{nm}}$ which corresponds to the emission peak of hemoglobin. Raw data were analyzed through a SoftMaxPro template and the IC50 calculated by fitting a 4 Parameter Logistic (4 PL) regression curve. The neutralization titer (IC50) is defined as the serum dilution giving 50% inhibition of hemolysis.

Data availability

The data supporting this work have been included as part of the article and the ESI.† Additional data can be made available on request.

Author contributions

CS, JC, MRR, FC and RA conceived the study; CS, BM, DYW, BB, CG, GA, and GR performed experimental work; CS, JC, IM, MRR, FC and RA analyzed the results; CS, JC, FC and RA wrote the manuscript; all revised the manuscript.

Conflicts of interest

BB, CG, GA, GR, IMR, MRR, FC and RA are employees of the GSK group of companies. CS and DYW participated in a post graduate studentship program at GSK. BM is a former GSK employee.

Acknowledgements

This work was sponsored by GlaxoSmithKline Biologicals SA and received funding from the European Union's Horizon 2020 research and innovation program under the Marie Skłodowska-Curie grant agreement no. 861194 (PAVax). The graphical abstract and Fig. 1, 2 and 4 were created with <https://www.BioRender.com>. Fig. 5 and S9† were created with GraphPad Prism. We thank the Formulation and ARC groups at GSK for the *in vivo* injections of the glycoconjugates.

References

- 1 E. Tacconelli, E. Carrara, A. Savoldi, S. Harbarth, M. Mendelson, D. L. Monnet, C. Pulcini, G. Kahlmeter, J. Kluytmans, Y. Carmeli, M. Ouellette, K. Outterson, J. Patel, M. Cavaleri, E. M. Cox, C. R. Houchens, M. L. Grayson, P. Hansen, N. Singh, U. Theuretzbacher, N. Magrini, A. O. Aboderin, S. S. Al-Abri, N. Awang Jalil, N. Benzonana, S. Bhattacharya, A. J. Brink, F. R. Burkert, O. Cars, G. Cornaglia, O. J. Dyar, A. W. Friedrich, A. C. Gales, S. Gandra, C. G. Giske, D. A. Goff, H. Goossens, T. Gottlieb, M. Guzman Blanco, W. Hryniewicz, D. Kattula, T. Jinks, S. S. Kanj, L. Kerr, M.-P. Kieny, Y. S. Kim, R. S. Kozlov, J. Labarca, R. Laxminarayan, K. Leder, L. Leibovici, G. Levy-Hara, J. Littman, S. Malhotra-Kumar, V. Manchanda, L. Moja, B. Ndoye, A. Pan, D. L. Paterson, M. Paul, H. Qiu, P. Ramon-Pardo, J. Rodriguez-Baño, M. Sanguinetti, S. Sengupta, M. Sharland, M. Si-Mehand, L. L. Silver, W. Song, M. Steinbakk, J. Thomsen, G. E. Thwaites, J. W. M. van der Meer, N. Van Kinh, S. Vega, M. V. Villegas, A. Wechsler-Fördös, H. F. L. Wertheim, E. Wesangula, N. Woodford, F. O. Yilmaz and A. Zorzet, *Lancet Infect. Dis.*, 2018, **18**, 318–327.
- 2 CDC, *2019 Antibiotic Resistance Threats Report*, U.S. Department of Health and Human Services, CDC, Atlanta, GA, 2019.
- 3 F. Micoli, F. Bagnoli, R. Rappuoli and D. Serruto, *Nat. Rev. Microbiol.*, 2021, **19**, 287–302.
- 4 A. Sharma, A. Krause and S. Worgall, *Hum. Vaccines*, 2011, **7**, 999–1011.
- 5 P. D. Lister, D. J. Wolter and N. D. Hanson, *Clin. Microbiol. Rev.*, 2009, **22**, 582–610.
- 6 R. M. Klevens, J. R. Edwards and R. P. Gaynes, *Clin. Infect. Dis.*, 2008, **47**, 927–930.
- 7 M. Klompas, Y. Khan, K. Kleinman, R. S. Evans, J. F. Lloyd, K. Stevenson, M. Samore and R. Platt, *PLoS One*, 2011, **6**, e18062.
- 8 A. Sandiumenge and J. Rello, *Curr. Opin. Pulm. Med.*, 2012, **18**, 187–193.



- 9 J. L. Veessenmeyer, A. R. Hauser, T. Lisboa and J. Rello, *Crit. Care Med.*, 2009, **37**, 1777–1786.
- 10 R. Kraemer, A. Blum, A. Schibler, R. A. Ammann and S. Gallati, *Am. J. Respir. Crit. Care Med.*, 2005, **171**, 371–378.
- 11 S. DeLeon, A. Clinton, H. Fowler, J. Everett, A. R. Horswill and K. P. Rumbaugh, *Infect. Immun.*, 2014, **82**, 4718–4728.
- 12 P. M. Alves, E. Al-Badi, C. Withycombe, P. M. Jones, K. J. Purdy and S. E. Maddocks, *Pathog. Dis.*, 2018, **76**, DOI: [10.1093/femspd/fty003](https://doi.org/10.1093/femspd/fty003).
- 13 J. Clegg, E. Soldaini, R. M. McLoughlin, S. Rittenhouse, F. Bagnoli and S. Phogat, *Front. Immunol.*, 2021, **12**, 705360.
- 14 R. Olaniyi, C. Pozzi, L. Grimaldi and F. Bagnoli, *Curr. Top. Microbiol. Immunol.*, 2017, **409**, 199–227.
- 15 H. Humphreys, K. Becker, P. M. Dohmen, N. Petrosillo, M. Spencer, M. van Rijen, A. Wechsler-Fördös, M. Pujol, A. Dubouix and J. Garau, *J. Hosp. Infect.*, 2016, **94**, 295–304.
- 16 C. Sorieul, M. Dolce, M. R. Romano, J. Codée and R. Adamo, *Expert Rev. Vaccines*, 2023, **22**, 1055–1078.
- 17 R. Rappuoli, *Sci. Transl. Med.*, 2018, **10**, eaat4615.
- 18 F. Khatun, I. Toth and R. J. Stephenson, *Adv. Drug Delivery Rev.*, 2020, **165–166**, 117–126.
- 19 G. Stefanetti, F. Borriello, B. Richichi, I. Zanoni and L. Lay, *Front. Cell. Infect. Microbiol.*, 2022, **11**, 808005.
- 20 N. Mohamed, Y. Timofeyeva, D. Jamrozy, E. Rojas, L. Hao, N. C. Silmon de Monerri, J. Hawkins, G. Singh, B. Cai, P. Liberator, S. Sebastian, R. G. K. Donald, I. L. Scully, C. H. Jones, C. B. Creech, I. Thomsen, J. Parkhill, S. J. Peacock, K. U. Jansen, M. T. G. Holden and A. S. Anderson, *PLoS One*, 2019, **14**, e0208356.
- 21 S. Jan, A. P. Fratzke, J. Felgner, J. E. Hernandez-Davies, L. Liang, R. Nakajima, A. Jasinskas, M. Supnet, A. Jain, P. L. Felgner, D. H. Davies and A. E. Gregory, *Front. Immunol.*, 2023, **14**, 1192821.
- 22 M. Anderluh, F. Berti, A. Bzducha-Wróbel, F. Chiodo, C. Colombo, F. Compostella, K. Durlík, X. Ferhati, R. Holmdahl, D. Jovanovic, W. Kaca, L. Lay, M. Marinovic-Cincovic, M. Marradi, M. Ozil, L. Polito, J. J. Reina, C. A. Reis, R. Sackstein, A. Silipo, U. Švajger, O. Vaněk, F. Yamamoto, B. Richichi and S. J. van Vliet, *FEBS J.*, 2022, **289**, 4251–4303.
- 23 F. Micoli, R. Adamo and P. Costantino, *Molecules*, 2018, **23**, 1451.
- 24 E. Saade, S. Gravenstein, C. J. Donskey, B. Wilson, B. Spiessens, D. Abbanat, J. Poolman, P. I. de Palacios and P. Hermans, *Vaccine*, 2020, **38**, 5100–5104.
- 25 J. Wassil, M. Sisti, J. Fairman, M. Davis, C. Fierro, S. Bennett, D. Johnson, T. S. Migone, K. Nguyen, P. Sauer, M. Currie, S. Iki and J. K. Simon, *Lancet Infect. Dis.*, 2024, **24**, 308–318.
- 26 R. M. Laird, Z. Ma, N. Dorabawila, B. Pequegnat, E. Omari, Y. Liu, A. C. Maue, S. T. Poole, M. Maciel, K. Satish, C. L. Gariepy, N. M. Schumack, A. L. McVeigh, F. Poly, C. P. Ewing, M. G. Prouty, M. A. Monteiro, S. J. Savarino and P. Guerry, *Vaccine*, 2018, **36**, 6695–6702.
- 27 H.-J. Kim, S. W. Na, H. A. Alodaini, M. A. Al-Dosary, P. Nandhakumari and L. Dyona, *Journal of Infection and Public Health*, 2021, **14**, 1864–1869.
- 28 B. J. Berube and J. Bubeck Wardenburg, *Toxins*, 2013, **5**, 1140–1166.
- 29 H. Zeng, F. Yang, Q. Feng, J. Zhang, J. Gu, H. Jing, C. Cai, L. Xu, X. Yang, X. Xia, N. Zeng, S. Fan and Q. Zou, *Vaccines*, 2020, **8**, 134.
- 30 R. P. Adhikari, H. Karauzum, J. Sarwar, L. Abaandou, M. Mahmoudieh, A. R. Boroun, H. Vu, T. Nguyen, V. S. Devi, S. Shulenin, K. L. Warfield and M. J. Aman, *PLoS One*, 2012, **7**, e38567.
- 31 H. Yu, J. Xiong, J. Qiu, X. He, H. Sheng, Q. Dai, D. Li, R. Xin, L. Jiang, Q. Li, Q. Chen, J. Peng, M. Wang, X. Rao and K. Zhang, *Front. Microbiol.*, 2020, **11**, 1971.
- 32 K. Inoue, M. Kinoshita, K. Muranishi, J. Ohara, K. Sudo, K. Kawaguchi, M. Shimizu, Y. Naito, K. Moriyama and T. Sawa, *Vaccines*, 2023, **11**, 1088.
- 33 P. Li, X. Wang, X. Sun, Z. Guan and W. Sun, *mSphere*, 2021, **6**, e0069921.
- 34 C. Wan, J. Zhang, L. Zhao, X. Cheng, C. Gao, Y. Wang, W. Xu, Q. Zou and J. Gu, *Front. Immunol.*, 2019, **10**, 781.
- 35 S. Hamaoka, Y. Naito, H. Katoh, M. Shimizu, M. Kinoshita, K. Akiyama, A. Kainuma, K. Moriyama, K. J. Ishii and T. Sawa, *Microbiol. Immunol.*, 2017, **61**, 64–74.
- 36 X. Wang, C. Liu, N. Rcheulishvili, D. Papukashvili, F. Xie, J. Zhao, X. Hu, K. Yu, N. Yang, X. Pan, X. Liu, P. G. Wang and Y. He, *npj Vaccines*, 2023, **8**, 76.
- 37 K. Peciak, E. Laurine, R. Tommasi, J.-w. Choi and S. Brocchini, *Chem. Sci.*, 2019, **10**, 427–439.
- 38 J. E. Edwards Jr, M. M. Schwartz, C. S. Schmidt, J. D. Sobel, P. Nyirjesy, F. Schodel, E. Marchus, M. Lizakowski, E. A. DeMontigny, J. Hoeg, T. Holmberg, M. T. Cooke, K. Hoover, L. Edwards, M. Jacobs, S. Sussman, M. Augenbraun, M. Drusano, M. R. Yeaman, A. S. Ibrahim, S. G. Filler and J. P. Hennessey Jr, *Clin. Infect. Dis.*, 2018, **66**, 1928–1936.
- 39 C. S. Schmidt, C. J. White, A. S. Ibrahim, S. G. Filler, Y. Fu, M. R. Yeaman, J. E. Edwards Jr and J. P. Hennessey Jr, *Vaccine*, 2012, **30**, 7594–7600.
- 40 M. Nanao, S. Ricard-Blum, A. M. Di Guilmi, D. Lemaire, D. Lascoux, J. Chabert, I. Attree and A. Dessen, *BMC Microbiol.*, 2003, **3**, 21.
- 41 M. Tontini, M. R. Romano, D. Proietti, E. Balducci, F. Micoli, C. Balocchi, L. Santini, V. Masignani, F. Berti and P. Costantino, *Vaccine*, 2016, **34**, 4235–4242.
- 42 T. Sawa, M. Kinoshita, K. Inoue, J. Ohara and K. Moriyama, *Antibodies*, 2019, **8**, 52.
- 43 R. Biemans, F. Micoli and M. R. Romano, in *Recent Trends in Carbohydrate Chemistry*, ed. A. P. Rauter, B. E. Christensen, L. Somsák, P. Kosma and R. Adamo, Elsevier, 2020, pp. 285–313, DOI: [10.1016/B978-0-12-820954-7.00008-6](https://doi.org/10.1016/B978-0-12-820954-7.00008-6).
- 44 S. Balan, J. W. Choi, A. Godwin, I. Teo, C. M. Laborde, S. Heidelberger, M. Zloh, S. Shaunak and S. Brocchini, *Bioconj. Chem.*, 2007, **18**, 61–76.
- 45 A. Schmidt, C. Jelsch, P. Østergaard, W. Rypniewski and V. S. Lamzin, *J. Biol. Chem.*, 2003, **278**, 43357–43362.
- 46 D. Voet, J. G. Voet and C. W. Pratt, *Fundamentals of biochemistry: Life at the molecular level*, John Wiley & Sons, Nashville, TN, 2016, 5th edn.
- 47 C. Pifferi, R. Fuentes and A. Fernández-Tejada, *Nat. Rev. Chem.*, 2021, **5**, 197–216.

